# The common nature of native iron in terrestrial rocks and meteorites: Microprobe and thermomagnetic data

**ARTICLE** *in* IZVESTIYA PHYSICS OF THE SOLID EARTH · SEPTEMBER 2015

Impact Factor: 0.4 · DOI: 10.1134/S1069351315050109



**4 AUTHORS:**

Diamar. Mihail. Pechersky

Russian Academy of Sciences

**52** PUBLICATIONS **553** CITATIONS

SEE PROFILE

Dilyara Kuzina

Kazan (Volga Region) Federal University

**10** PUBLICATIONS **15** CITATIONS

SEE PROFILE

Danis Nourgaliev

Kazan (Volga Region) Federal University

**66** PUBLICATIONS **390** CITATIONS

SEE PROFILE

Vladimir Anatolevich Tselmovich

Russian Academy of Sciences

**58** PUBLICATIONS **147** CITATIONS

SEE PROFILE

ISSN 1069-3513, Izvestiya, Physics of the Solid Earth, 2015, Vol. 51, No. 5, pp. 748–763. © Pleiades Publishing, Ltd., 2015.
Original Russian Text © D.M. Pechersky, D.M. Kuzina, D.K. Nurgaliev, V.A. Tsel'movich, 2015, published in Fizika Zemli, 2015, No. 5, pp. 140–155.

# The Common Nature of Native Iron in Terrestrial Rocks and Meteorites: Microprobe and Thermomagnetic Data

**D. M. Pechersky[a], D. M. Kuzina[b], D. K. Nurgaliev[b], and V. A. Tsel'movich[a]**

[a] *Schmidt Institute of Physics of the Earth, Russian Academy of Sciences, ul. Bol'shaya Gruzinskaya 10, Moscow, 123995 Russia*

*e-mail: diamarmp@gmail.com*

[b] *Kazan Federal University, ul. Kremlyovskaya 18, Kazan, Republic of Tatarstan, 420008 Russia*

Received March 2, 2015

**Abstract**—The microprobe and thermomagnetic data for native iron in terrestrial rocks (xenoliths from mantle hyperbasites, Siberian traps, and oceanic basalts) are generalized and compared to the data for native iron from sediments and meteorites. It is found that the native iron particles contained in the continental and oceanic hyperbasites and basites are similar in composition, shape, and grain size. These particles are predominantly nickel-free and similar to the extraterrestrial iron from sediments and meteorites. This similarity suggests the similar sources of origin of these particles. This means that the terrestrial conditions were close to the conditions that existed at the source planets of the meteorites, e.g., the bodies from the asteroid belt which have been subsequently disintegrated, and crushed into cosmic interplanetary dust, which has entered the terrestrial sediments. This similarity originates from the homogeneity of the gas-dust cloud at the early stage of the Solar System. The predominance of extraterrestrial native iron in sediments is accounted for by the fact that the interplanetary dust is mainly contributed by the material from the upper mantle of the source planets of cosmic dust.

**DOI:** 10.1134/S1069351315050109

## INTRODUCTION

Metal particles in sediments are dominated by nickel-free native iron. We have come to this conclusion based on a long study of the composition and distribution of native iron particles in sediments by microprobe and thermomagnetic analyses (Pechersky et al., 2006; Pechersky et al., 2006; 2008; 2009; 2011; 2012; 2013a; 2013b; 2013c; Pechersky, 2010; Pechersky, 2012; Pechersky and Sharonova, 2012; 2013; Markov et al., 2015; Pechersky and Kuzina, 2015). These studies cover 30 sedimentary objects (collections of B.Z. Asanidze, V.G. Bakhmutov, A.F. Grachev, A.Yu. Kazanskii, O.A. Korchagin, M.I. Kuz'min, E.A. Molostovskii, I.O. Murdmaa, D.P. Naidin, V.E. Pavlov, V.M. Trubikhin, V.A. Fomin). One of the probable explanations is that Ni-free native iron originated from the mantle rocks of the asteroid belt as a result of their being crushed (McFadden et al., 2007; Pechersky and Kuzina, 2015). For solving this problem, in the present work, we have additionally selected and analyzed a series of other samples, besides the sediments. Firstly, it is the samples of the terrestrial mantle ultrabasic rocks transported onto the surface of the Earth by basaltic lavas. They include mantle xenoliths from the lavas in the Antarctic, Primor'e, Mongolia, Syria, Svalbard (A.Ya. Saltykovskii's collection), and Vitim Plateau (I. Ashchepkov's collection). Secondly, it is the trap samples—igneous rocks of knowingly terrestrial origin, widespread on continents, in our case on the Siberian Platform (A. Latyshev's collection). The collection includes samples from two sills in the Angara province, from ten lava flows of the Maymecha–Kotui province, and from four flows of Norilsk province; the trap bodies have different thickness varying from 2 to 20 m and larger. Several samples were taken from the tuff layer confined between the lava flows of the Norilsk province. Thirdly, there are 21 samples from the widespread oceanic basalts forming the floor of the World Ocean. In our case these are the samples from the Atlantic (13), Pacific (5), and Indian (1) oceans and the Red Sea (2) (collections of V. Matveenkov and S. Silant'ev). We compare these data to the analogous microprobe and thermomagnetic results for the meteorites described in (Pechersky et al., 2012; Markov et al., 2015).

## METHODS

The microprobe analysis (MPA) and other microscopic studies were carried out at the Borok Geophysical Observatory of the Schmidt Institute of Physics of the Earth of the Russian Academy of Sciences. The MPA measurements were conducted by V.A. Tsel'movich on the Tescan Vega 2 microprobe with an X-ray energy-dispersive spectrometer. The samples intended for microprobe analysis were disintegrated by ultrasound, after which the magnetic frac-

**Table 1.** The number of the native iron particles of different composition and Ni particles

| | *N* | S | Fe | Si | Al | Ti | Cr | Mg | Other | FeNi | Ni |
|---|---|---|---|---|---|---|---|---|---|---|---|
| Sediments, total | 105 | 552 | 388 | 286 | 108 | 29 | 102 | 53 | 39 | 99 | 65 |
| | % | | 70 | 52 | 20 | 5 | 18 | 10 | 7 | 18 | 12 |
| Xenoliths | 16 | 166 | 128 | 80 | 25 | 23 | 22 | 53 | 10 | 23 | 16 |
| | % | | 77 | 48 | 15 | 14 | 13 | 32 | 6 | 14 | 10 |
| Vitim | 3 | 28 | 27 | 21 | 4 | 5 | 8 | 7 | 0 | 1 | 0 |
| Mongolia | 2 | 22 | 14 | 5 | 5 | 0 | 0 | 4 | 0 | 2 | 6 |
| Primor'e | 7 | 72 | 57 | 36 | 10 | 14 | 7 | 24 | 9 | 10 | 5 |
| Syria | 3 | 33 | 23 | 11 | 6 | 5 | 6 | 16 | 1 | 5 | 5 |
| Antarctic | 1 | 11 | 6 | 7 | 0 | 0 | 1 | 2 | 0 | 5 | 0 |
| Traps, total | 21 | 81 | 72 | 40 | 12 | 5 | 12 | 14 | 21 | 1 | 8 |
| | % | | 89 | 49 | 15 | 6 | 15 | 17 | 26 | 1.2 | 10 |
| Angara | 6 | 23 | 22 | 15 | 7 | 3 | 3 | 3 | 6 | 0 | 1 |
| Maymecha | 11 | 33 | 26 | 14 | 3 | 2 | 8 | 7 | 12 | 1 | 6 |
| Norilsk | 2 | 7 | 5 | 6 | 0 | 0 | 3 | 2 | 3 | 0 | 2 |
| Tuff layer | 1 | 9 | 9 | 5 | 0 | 0 | 0 | 0 | 1 | 0 | 0 |
| Oceanic basalts, total | 14 | 79 | 67 | 29 | 28 | 10 | 19 | 8 | 33 | 8 | 4 |
| | % | | 85 | 38 | 35 | 13 | 24 | 10 | 42 | 10 | 5 |
| Meteorites, total | 44 | 896 | 68 | 50 | 34 | 0 | 2 | 18 | 18 | 823 | 5 |
| | % | | 8 | 6 | 4 | 0 | 0.2 | 2 | 2 | 92 | 0.6 |

*N* is the number of samples in a given group of the rocks; Σ is the total number of native iron and nickel particles (Fe+ FeNi + Ni) in a given group of the rocks; Fe is the number of Ni-free native iron particles; Si, Al, Ti, Cr, Mg are the number of iron particles containing one of the indicated elements; *other* means the other admixture elements in iron particles (Mn, P, S, etc.); FeNi is the number of kamacite particles and other FeNi alloys and the alloys with more complex composition; Ni is the number of native nickel particles; % is the percentage of iron particles containing the admixtures of different elements with respect to Σ.

tion was extracted from the material by a permanent magnet. The MPA measurements were conducted with an accelerating voltage of 20 kV and a beam current of 0.2 nA. The diameter of the probe was ~0.2 μm, and the size of the analyzed area was 2 μm.

The thermomagnetic analysis (TMA) included the measurements of magnetization in the samples in the magnetic field of 400 mT and the temperature dependences of magnetization in the temperature interval from 20 to 800°C. The TMA measurements were conducted at the paleomagnetic laboratory of the Kazan State University by D.M. Kuzina using the Curie express balance. The temperature limit was specified at 800°C in order to overlap the Curie points of native iron, which may reach 770°C (pure iron). As of now, TMA is the only method suitable for the fast and mass estimation of the magnetic mineral content without extracting these minerals from the rock. The Curie points are estimated as accurately as within 5–10°, and the magnetic moment, within $3 \times 10^{-8}$ Am$^2$. The accuracy of the magnetic mineral content is rather low; however, this is not critical compared to the background fluctuations in the native iron content in the studied rocks, which may attain a few orders of magnitude. The losses in accuracy are counterbalanced by the simplicity of the TMA method itself, a fast procedure for preparing the samples and obtaining the data.

In most cases, the results of MPA and TMA agree in the composition of the magnetic minerals (iron, titanomagnetite, and magnetite) but the estimates of the iron content have significant discrepancies. This is due to the fact that TMA uses a tiny specimen whose weight is less than 0.1 g, whereas MPA is conducted with the enriched magnetic fraction extracted from a larger piece of the rock.

## MPA DATA

The main results of MPA for the sediments, xenoliths, traps, oceanic basalts, and meteorites are presented in Table 1 and in Figs. 1 to 11 illustrating the comparison of the compositions, shapes, and grain sizes of the native iron particles.

### *Composition*

Most of the particles detected by MPA in the sediments, xenoliths, traps, and oceanic basalts are pure iron and iron with different admixtures except Ni. The sediments contain 18% FeNi alloy particles. The per-

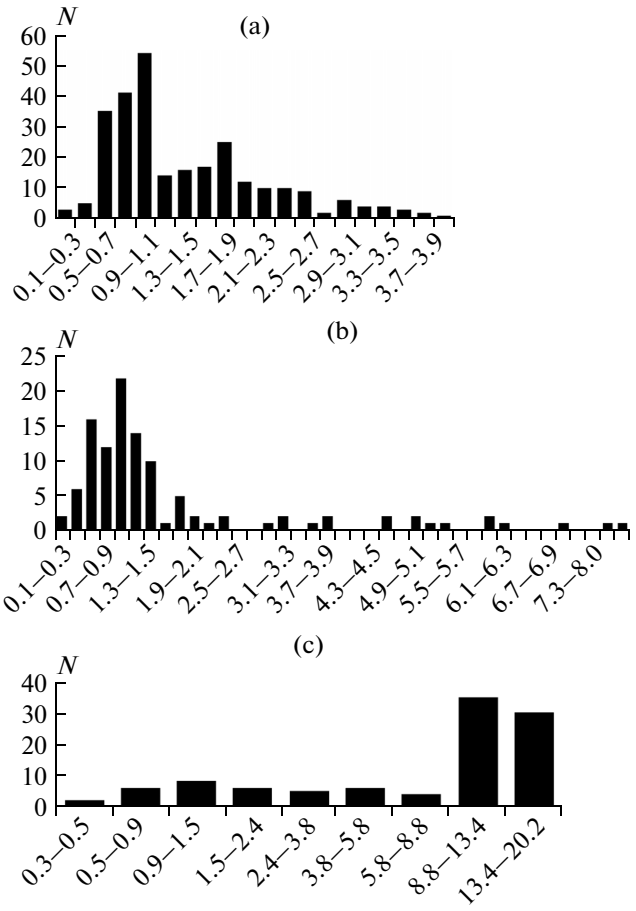


**Fig. 1.** Concentrations of the (a) silica, (b) aluminum, and (c) chrome admixtures in the particles of native iron from sediments according to MPA. Concentrations are in wt %; *N* is the number of the iron particles containing a given admixture.

centage of FeNi particles is 14% in xenoliths and 10% in the oceanic basalts, whereas only a single FeNi grain has been identified in the traps (Table 1). For comparison, Ni-free iron in the meteorites makes up 8%, whereas the remaining 92% are FeNi alloys containing from a few percent to 50% and more of Ni, as well as schreibersite and other alloys with a more complex composition (Tables 1 and 2) (Pechersky et al., 2012). Thus, the distribution of the FeNi alloys across the section of the Earth has a distinct trend, decreasing from the high clearly predominant FeNi content in the bottom mantle and core (92%) to their relatively low fraction in the upper mantle (14%) and in the basic igneous rocks (10%), both intrusive and volcanic, crystallized within the earth crust and on its surface. This scheme does not describe the distribution of native nickel. The latter makes up 5–12% in the sediments, xenoliths, traps, and oceanic basalts (Table 1), and only three meteorites contain single individual grains of native Ni (Pechersky et al., 2012). At the same time, the Ni grains occurring in sediments and xenoliths have varying sizes, whereas the Ni grains in traps and oceanic basalts are small and typically confined to the carbon-rich localities.

The admixtures are ubiquitous and have similar distributions in all the rock groups (Table 1, Figs. 1–5). The Si admixture in native iron is most common; it is detected in all the studied samples (Table 1, Figs. 1a, 2a, 3a, 4a, and 5a). The concentration of this admixture reaches 3–4%, and its distribution reflects the neighboring silicates captured by the probe. Most samples contain modes which probably reflect an isomorphic Si admixture in the iron particles (Figs. 1a, 2a, 3a, 4a, and 5a), since it is barely possible that an element captured from a neighboring grain has a constant concentration. The aluminum admixture is mainly below 1–1.5%. It is minimal in traps (Fig. 3b), about 3–4% in xenoliths (Fig. 2b), oceanic basalts (Fig. 4b), and meteorites (Fig. 5b), and as high as 9% in sediments (Fig. 1b). The Si and Al concentrations are closely correlated ($r = 0.87$) reflecting the fact that a significant fraction of the detected Al again comes from the neighboring silicates captured by the microprobe. The chrome admixture in iron particles from sediments, traps, and basalts makes up two groups (Figs. 1c, 3c, and 4c). The samples of the first group contain 0.1–6% Cr without a clear mode; the second group contains 8–20% Cr with the mode in the 9–13% interval. Typically, the Cr admixtures in xenoliths exceptionally pertain to the first group with mode 0.3–0.5% Cr (Fig. 3c). This distribution of Cr admixtures probably reflects the different formation conditions of these two groups of particles. Titanium is present in 5–

**Table 2.** Native iron and FeNi alloys in meteorites

| Meteorites | *N* | Σ | Fe | FeNi | Schr |
|---|---|---|---|---|---|
| Stone | 14 | 231 | 34 | 197 | 6 |
| | | % | 14.7 | 85.3 | 2.6 |
| Iron (iron + iron-stone) | 15 | 534 | 68 | 466 | 90 |
| | | % | 12.7 | 87.3 | 16.8 |

*N* is the number of samples; Σ is the total number of native iron particles and FeNi alloys (kamacite, taenite, etc.); Fe is the number of Ni-free native iron particles; FeNi is the number of particles of FeNi alloys; Schr is the number of schreibersite particles $(Fe, Ni)_3P$; % is the percentage of Ni-free iron particles, FeNi alloys, and schreibersite with respect to the total number Σ.

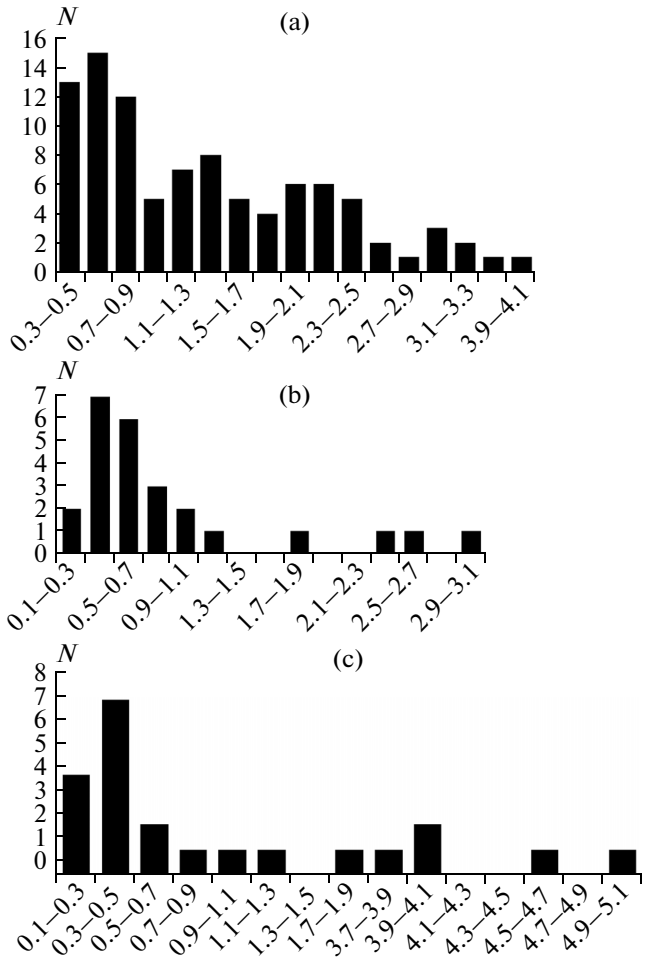


**Fig. 2.** Concentrations of the (a) silica, (b) aluminum, and (c) chrome admixtures in the particles of native iron from xenoliths according to MPA. Concentrations are in wt %; *N* is the number of the iron particles containing a given admixture.

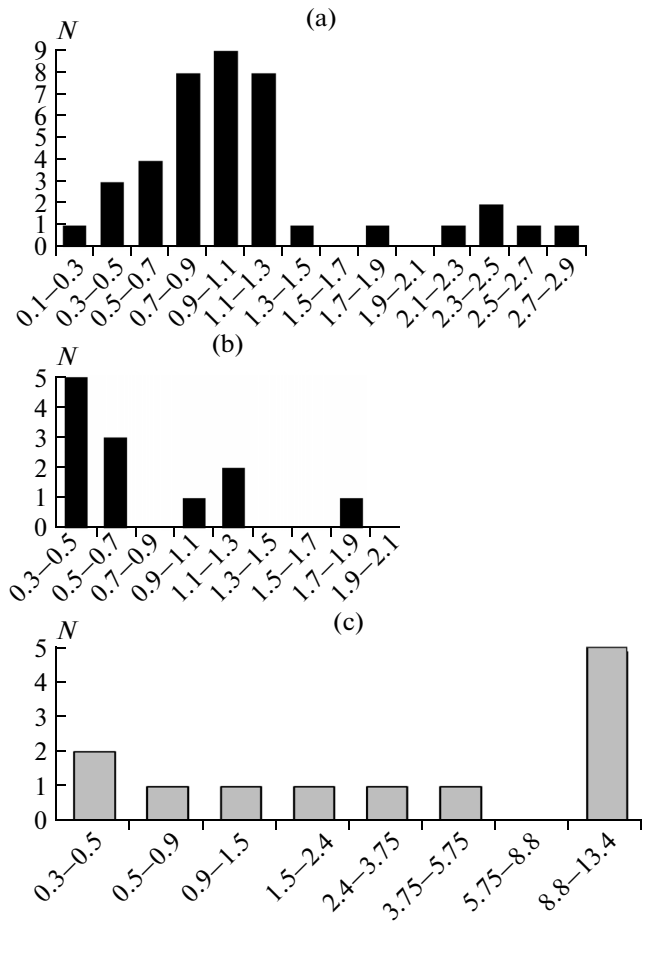


**Fig. 3.** Concentrations of the (a) silica, (b) aluminum, and (c) chrome admixtures in the particles of native iron from traps according to MPA. Concentrations are in wt %; *N* is the number of the iron particles containing a given admixture.

14% of the iron particles in the sediments, traps, and oceanic basalts (Table 1) and is nonuniformly distributed across the objects. For example, the Ti admixture in xenoliths is absent in the iron particles from Antarctic and Mongolia, whereas its content in the other objects is up to 18% (Table 1). The Ti concentration in iron particles varies from 0.2 to 9%. Titanium is not detected in iron from the studied meteorite samples (Table 1) (Pechersky et al., 2012). Iron particles from oceanic basalts often contain manganese (8–10%), which typically cooccurs with chrome. In our opinion, the high presence of the Ti- and, particularly, Mn-containing particles in xenoliths is due to the contamination of xenolith material by the hosting basalts. This conclusion also follows from the high concentration of titanomagnetite in a number of xenolith samples, untypical of the mantle hyperbasites and related to the basalts hosting the xenoliths. The MPA of xenolith samples revealed 43 titanomagnetite grains with the Ti content varying from 8 to 18% (average 12.5%). The results of MPA are supported by TMA (see the TMA section of this paper and Fig. 12). Abundant titanomagnetite grains are detected in traps and oceanic basalts. These grains contain 7–17% Ti; the average Ti content in the traps and oceanic basalts is 8.7 and 10.5%, respectively. The titanomagnetite grains detected in traps are frequently large and quite clearly faceted, whereas the titanomagnetite grains in the oceanic basalts have skeletal forms, indicative of their crystallization during very fast lava cooling, up to the predominance of the vitrified material.

Thus, we may reliably state that particles of native iron, both pure and containing different admixtures except for Ni, have a widespread (global) distribution. The iron particles have similar compositions in the sediments, hyperbasites, basalts (oceanic and continental), and meteorites.

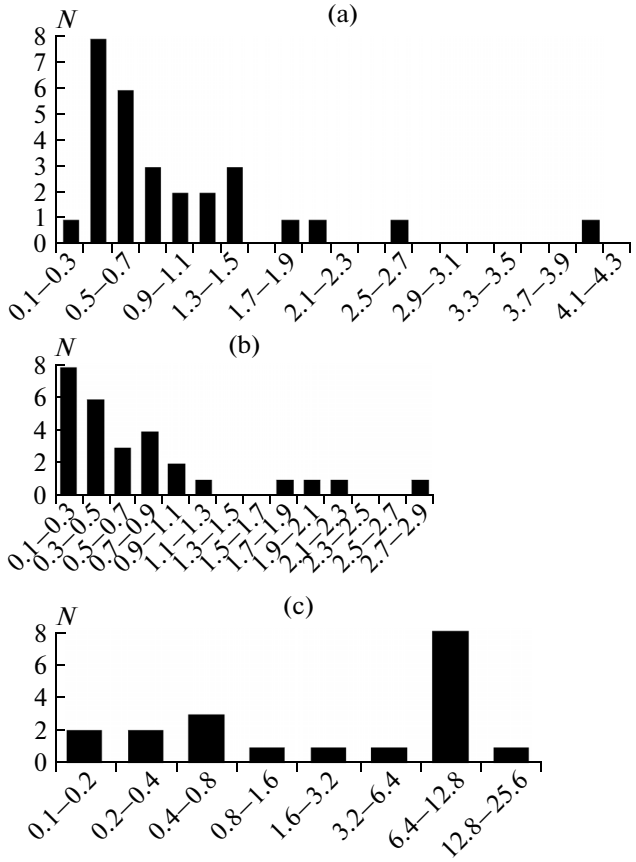


**Fig. 4.** Concentrations of the (a) silica, (b) aluminum, and (c) chrome admixtures in the particles of native iron from oceanic basalts according to MPA. Concentrations are in wt %; *N* is the number of the iron particles containing a given admixture.

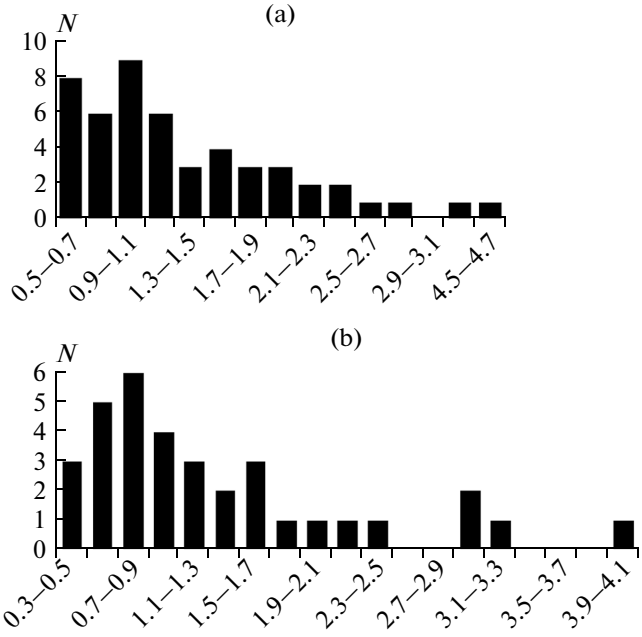


**Fig. 5.** Concentrations of the (a) silica and (b) aluminum admixtures in FeNi alloy from stone meteorites according to MPA. Concentrations are in wt %; *N* is the number of the iron particles containing a given admixture.

### *Shape and Grain Size of Iron Particles*

The great bulk of native iron particles in sediments (Fig. 6), xenoliths (Fig. 7), traps (Fig. 8), oceanic basalts (Fig. 9), and meteorites (Fig. 10) have identical, complicated configurations (angular forms, chips, flakes, spiral structures, dendrites, etc.). This probably reflects the monotonic, primarily igneous formation conditions or, in other words, the common origin of these particles, which got into the sediments. Native iron particles with spherical shapes are extremely rare. In particular, they form clusters rather limited in size, e.g., as in the *K/T* boundary layer in the Gams deposits (Grachev et al., 2009).

The distributions of native iron particles in the sediments, xenoliths, traps, and basalts are fairly similar. The grain sizes vary widely from a submicron to 300–600 μm with the same mode in the interval of 10 to 20 μm in all the groups of rocks from different regions (Fig. 11). This applies to the native iron particles with Ni and within Ni admixture (Figs. 11a and 11b). The predominant species have a size of up to 100 μm, characteristic of the extraterrestrial particles which mostly survive after passing through the Earth's atmosphere (Florenskii, 1965), whereas particles larger than 100 μm are almost completely burned out. The particles with sizes of above 100 μm, which occur in the sediments, are most likely to be the products of the meteorite falls rather than interplanetary dust. For example, there are sedimentary objects where the larger sizes are mainly characteristic of Ni-free species (e.g., in the Himalaya), while in the other objects, in contrast, Ni-bearing particles are larger than the Ni-free ones (e.g., Podol'e), probably mainly reflecting the remoteness or closeness of the studied object to the meteorite fall site (Korchagin, 2013; Pechersky and Kuzina, 2015). This only relates to the extraterrestrial particles in sediments and by no means explains in it the similar distribution in the case of iron particles from the Earth's mantle and the crust, not related to the interplanetary dust. It is likely that the range of the grain sizes of iron particles is determined by the conditions in their source—the mantle and crustal igneous rocks such as mantle hyperbasites (xenoliths) and basalts (continental traps and oceanic basalts). The crystallization conditions of native iron particles are also reflected in the tails of the histograms: the largest species up to 600 μm occur in hyperbasites with a characteristic slow crystallization (Fig. 11b); and the smaller particles (up to 100 μm) are related to the rapidly crystallizing lava flows (Fig. 11c) and submarine lava eruptions (Fig. 11d). In contrast, everything may get into the sediments; however, the large particles

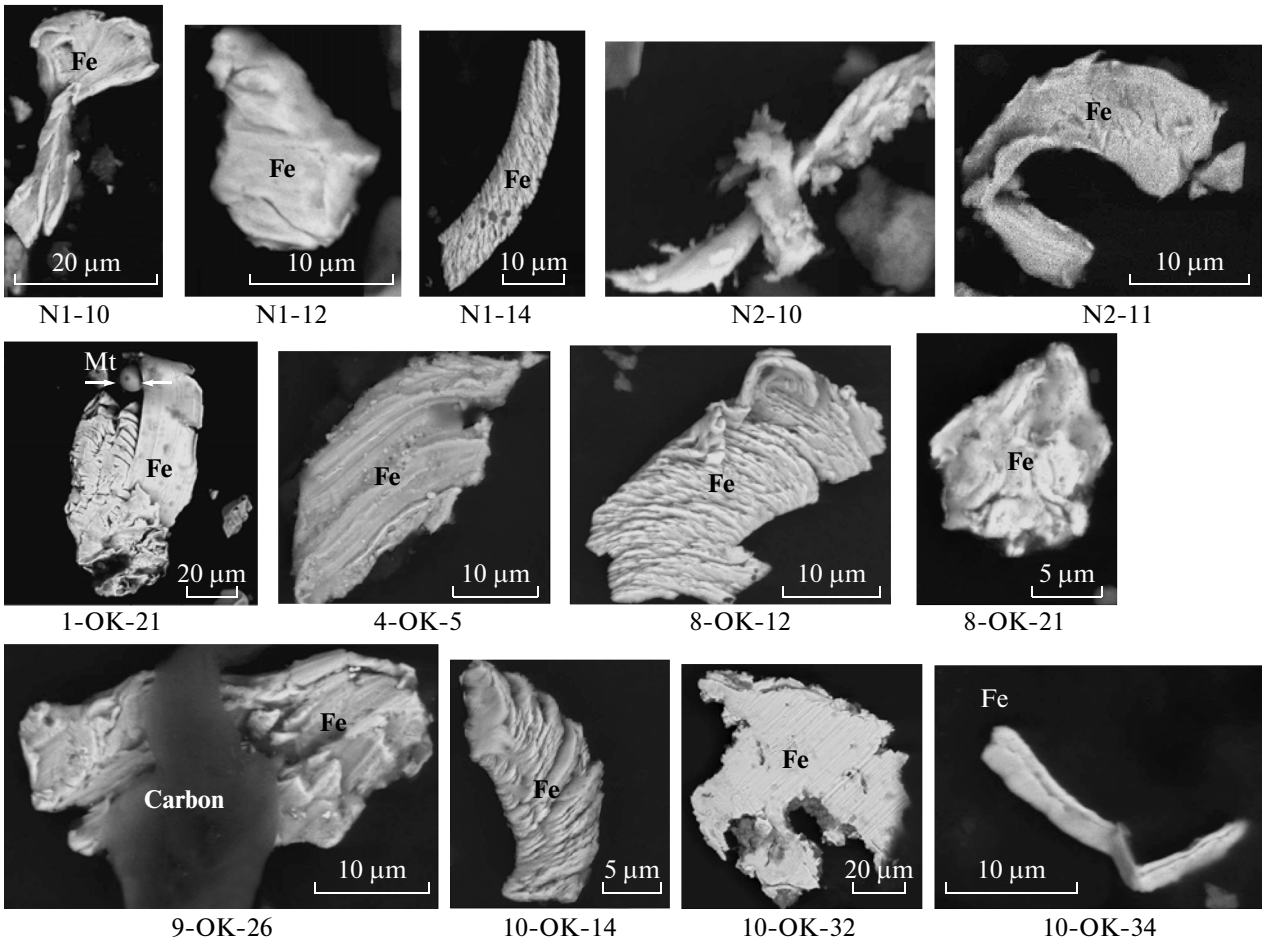


**Fig. 6.** The grain shapes of native iron in sediments.

coming from space get burned out, as noted above (Fig. 11a).

## TMA DATA

The results of TMA for the sedimentary rocks and meteorites are presented in a number of the papers cited in the Introduction. Here we consider the TMA data for xenoliths, traps, and oceanic basalts. The examples of the results of TMA are shown in Fig. 12 and in the histogram of the Curie points in Fig. 13. The hyperbasites (xenoliths) and volcanic glass of the oceanic basalts typically have a hyperbolic $M(T)$ curve (Figs. 12a, 12k, and 12l). This curve indicates clearly predominant paramagnetic iron-bearing minerals such as olivine and pyroxene. The magnetite and titanomagnetite concentration in the hyperbasite samples is below 0.1% (Figs. 12a, 12c, 12e), barely sufficient to distort the hyperbolic shape of the $M(T)$ curve. Parabolic ($Q$-type) $M(T)$ curves, indicative of a high percentage of titanomagnetite and magnetite, are very rare. Titanomagnetite has the Curie points ranging from 220 to 400°C (Figs. 12a, 12c, 12 e), consistent with the titanomagnetite compositions identified by MPA. Titanomagnetite is untypical of hyperbasites, and we attribute its occurrence to the contamination of xenolith material by the hosting basalts; i.e., they are irrelevant for our study.

Among the 50 xenolith samples studied, the Curie points of iron (700–770°C, Figs. 12b, 12h, 12j, and 12l) are only revealed in ten samples (Fig. 13b). This feature distinguishes these samples from the sediments where iron particles are almost ubiquitous. According to TMA, the iron concentration varies from <0.0001 to 0.003%; the average iron content in ten samples is 0.00076%.

The pattern of TMA data for the traps is slightly different. The $T(M)$ curves are all of the parabolic shape ($Q$-type, e.g., Fig., 12g). In these rocks, the concentration of titanomagnetites and their secondary magnetites is significantly higher, which is typical of most basalt types. In our traps, the traces of titanomagnetite have only been preserved in three samples, where their concentration is 0.06–0.3% (e.g., Fig. 12g). Magnetite is present in all the studied sam-

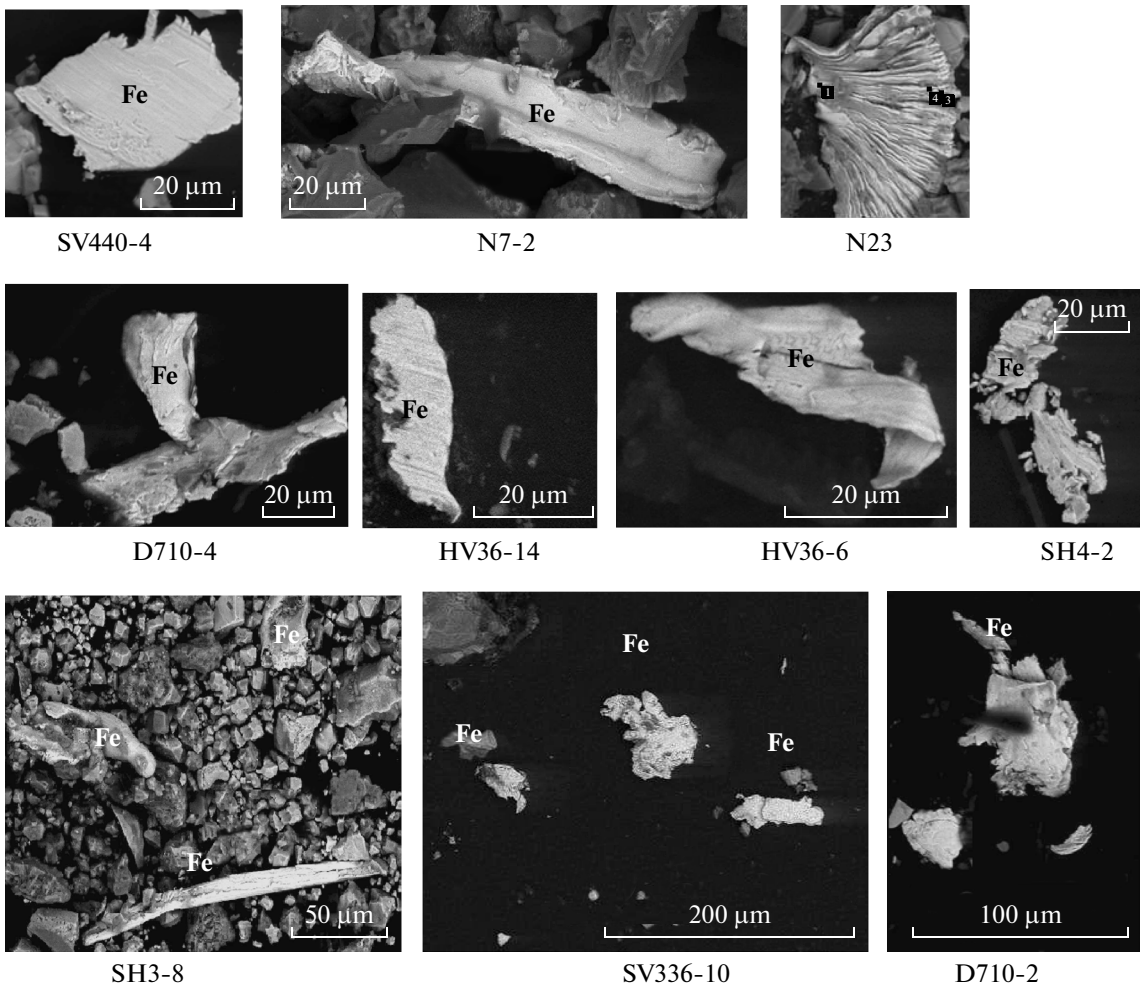


**Fig. 7.** The grain shapes of native iron in the mantle xenoliths.

ples; its concentration varies from 0.01 to 5% with the average concentration of ~2%.

Just as in hyperbasites, the distribution of iron particles in traps is nonuniform. Iron is more abundant in sills; there are flows where iron particles are not detected by TMA, and neither are they detected in tuffs. Iron in traps is much more common than in hyperbasites (xenoliths): iron is established in 18 of the 37 studied samples (Fig. 13c). Its percentage in these samples varies from 0.0001 to 0.0055%; the average content in these 18 samples is 0.0012%. The distribution of the Curie points is very similar to hyperbasites (Figs. 13b and 13c): iron grains are dominated by pure iron and a close iron species with $T_c = 740–760°C$ (Fig. 13c).

The specificity of submarine lava flows is reflected in the $M(T)$ curves. Firstly, these curves are typically hyperbolic due to the prevailing paramagnetic forms of the iron compounds. Therefore, titanomagnetite grains had not yet been formed in these objects at the time of the lava outflow. As follows from the microscopic observations, the studied oceanic basalts (even significantly crystallized, close to dolerites) are dominated by skeletal forms of titanomagnetite grains (Fig. 9, e.g., samples 2750-3-3, P72-4-5, and P72-4-6). Secondly, titanomagnetites mainly have relatively low Curie points (200–400°C, e.g., Fig. 12i) and low concentrations of secondary magnetite up to its full absence: the lava is cooling too fast to allow titanomagnetite to get oxidized to magnetite. Noticeable oxidation of titanomagnetite with the formation of magnetite is typical of the slowly cooling thick lavas, trap sills, and the bodies of the mantle hyperbasites (a typical example is shown in Fig. 12g).

By the emergence conditions of native iron, oceanic basalts are no different from the other terrestrial igneous formations. Therefore, iron particles in them have been formed *before* the effusion, and the conditions of their emergence are similar to those for the iron particles from traps and hyperbasites. Iron particles in the oceanic basalts are even more common than in traps: out of the 21 samples, native iron is detected in 14 samples. In these samples, the iron concentration varies from 0.0002 to 0.018% with an average

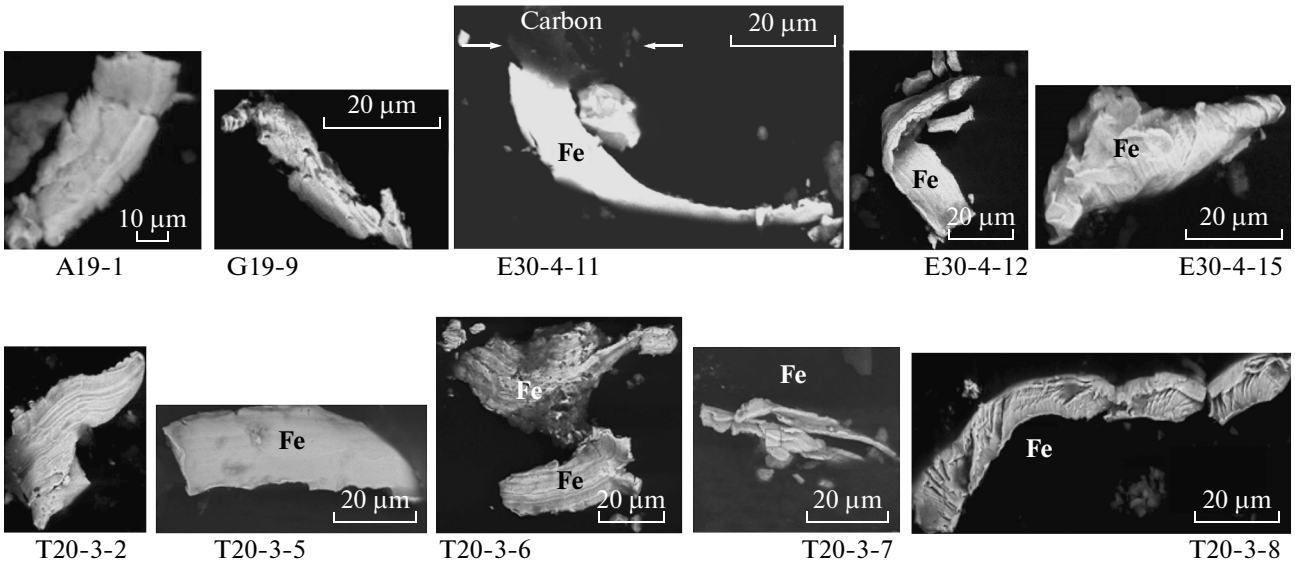


**Fig. 8.** The grain shapes of native iron in traps.

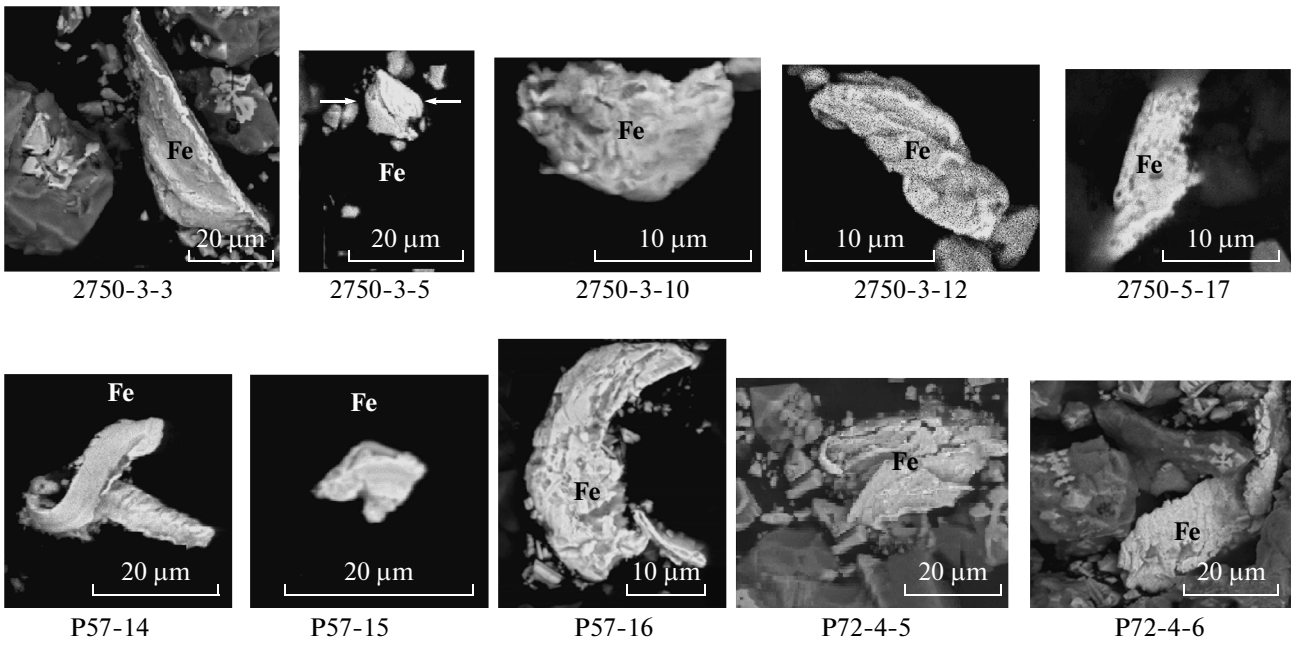


**Fig. 9.** The grain shapes of native iron in the oceanic basalts.

0.0009%. The histograms of the Curie points of the oceanic basalts, traps, and hyperbasites are almost identical (Figs. 13b, 13c, and 13d).

Occurrences of native iron with $T_c = 730–760°C$ (Fig. 13d) are relatively more frequent in sediments compared to the other groups of the terrestrial rocks. The fraction of these particles significantly increases in the meteorites (Fig. 13d). Thus, the histograms of the Curie points for the terrestrial rocks (xenoliths, traps, and oceanic basalts) noticeably differ from the histograms of the meteorites (i.e., of extraterrestrial native iron). The histograms of the Curie points for the sediments sum up the histograms for terrestrial and extraterrestrial native iron (Fig. 13).

The bulk of the particles, according to MPA, are pure iron and iron with the admixtures of silica, aluminum, chrome, etc., but not nickel (Table 1). Correspondingly, the Curie points below 770°C detected by TMA are accounted for by the admixtures which are present in the iron particles. For example, the presence of 2% of Si reduces the Curie point to 750°C, and a 4% Si admixture diminishes it to 720°C. With a

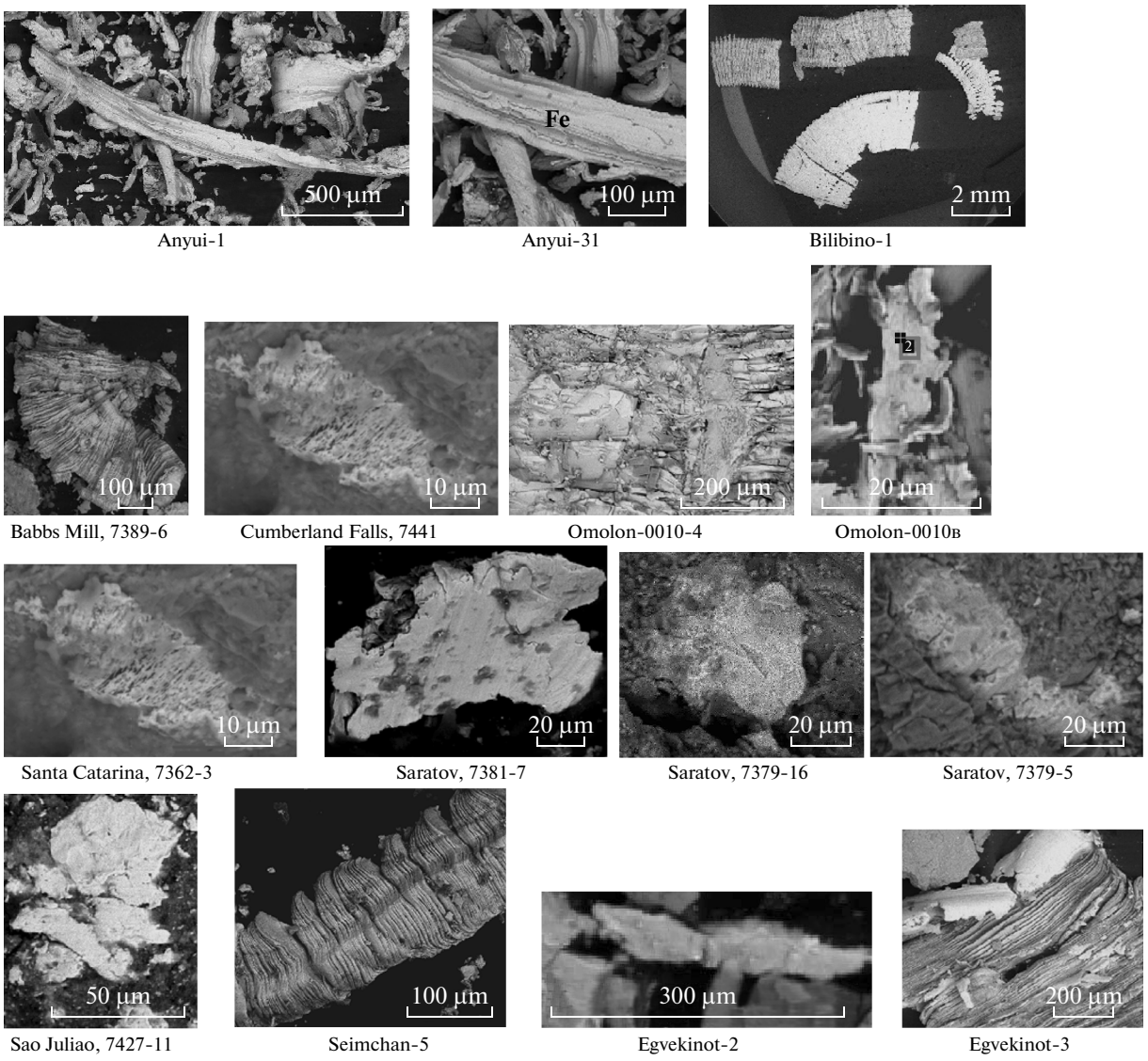


**Fig. 10.** The grain shapes of native iron in the stone meteorites.

5% Cr admixture, the Curie point drops to 750°C and with a 10% Cr admixture it is 728°C. A 2% aluminum admixture decreases the Curie point of native iron to 760°C (Bozorth, 1951).

Native nickel grains are identified in 5–12% of metal particles (and 0.6% in the meteorites) (Table 1). As a rule, they occur as single particles, frequently confined to the accumulations of carbon-bearing material. Nickel is perfectly identified by $T_c = 358$°C; however, among the numerous thermomagnetic measurements in the sediments, hyperbasites, traps, oceanic basalts, and meteorites, nickel has only been reliably detected in a single tiny specimen from the boundary layer of the Gams section (Grachev et al., 2009; Pechersky et al., 2006) and less reliably in a few rare cases (Fig. 12f). Hence, in the samples where Ni particles are detected by MPA but not identified by TMA, their amount is below the TMA sensitivity; i.e., the concentration is below $10^{-3}$%.

## DISCUSSION

The first striking feature that has to be mentioned is the similarity in the compositions, shapes, and grain sizes of the native iron particles in hyperbasites (xenoliths), traps, oceanic basalts, and meteorites. Their likeness to the iron particles in sediments indicates that these rock types can be the sources of native iron in sediments; i.e., it indicates these particles have terrestrial origin even in sediments. However, this conclusion is challenged by two facts. The first is the close similarity in the compositions, shapes, and grain sizes of these particles to the objects that are surely extraterrestrial—meteorites. The second fact is the global dis-

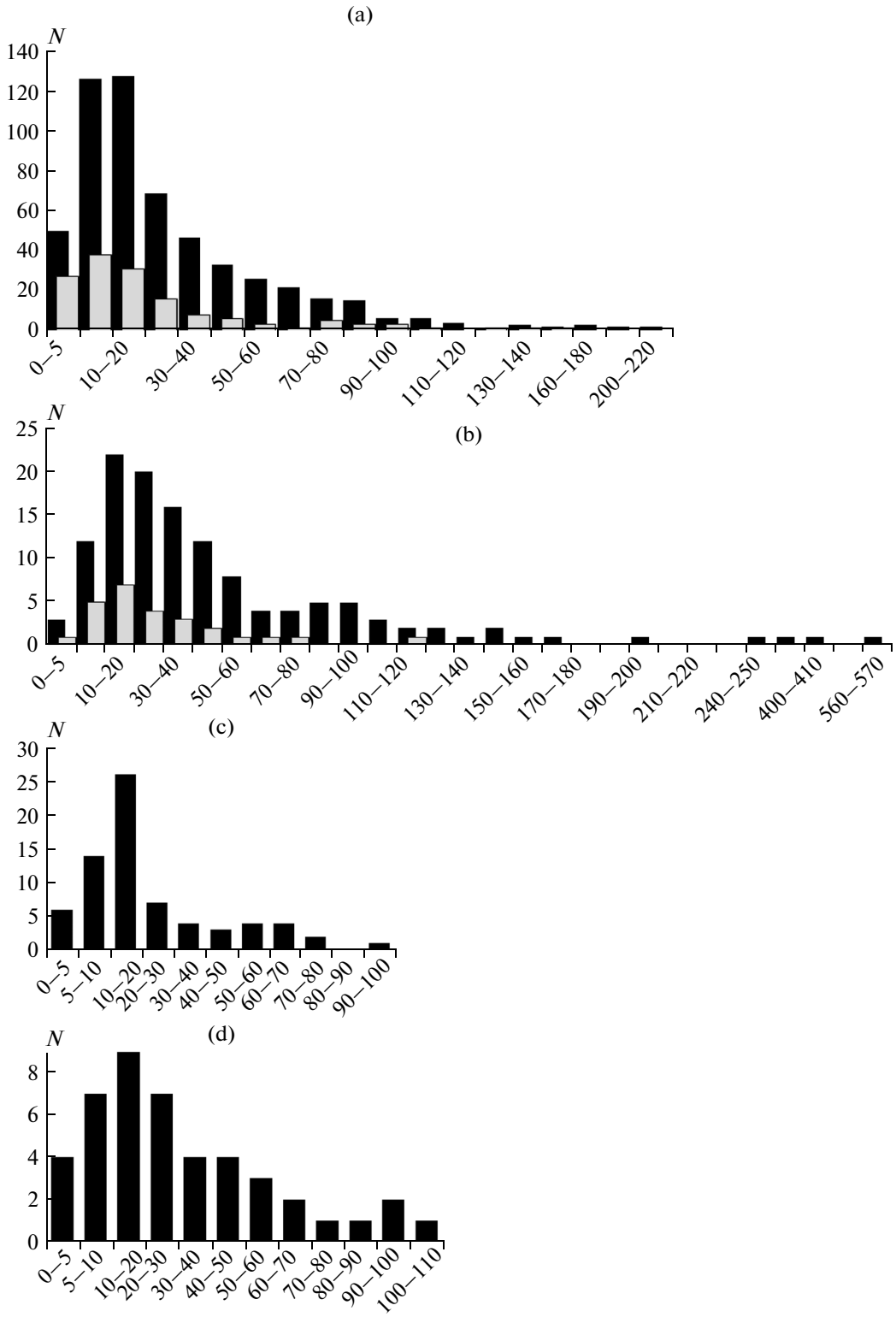


**Fig. 11.** The grain size of native iron (in μm) with Ni (gray) and without Ni (black) in the (a) sediments; (b) xenoliths, (c) traps, and (d) oceanic basalts.

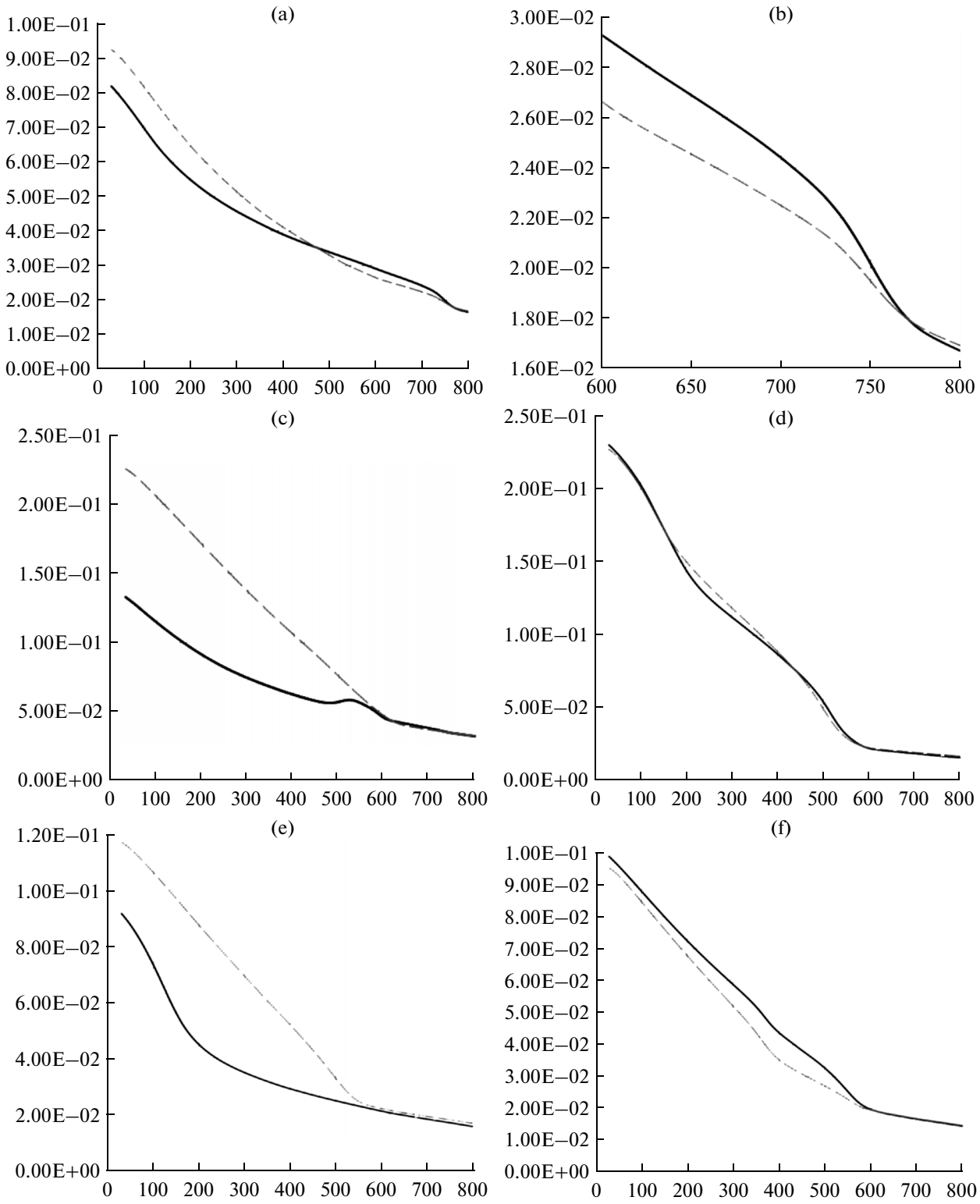


**Fig. 12.** The examples of the results of TMA: (a), (b), sample CSV-462, lherzolite xenolith, Sorochinskii Volcano: (a), thermal curves in the temperature interval from 20 to 800°C; (b), the high-temperature segment of the curve; (c), sample SV-6, lherzolite xenolith, Sorochinskii Volcano; (d), sample SV501, lherzolite xenolith, Sorochinskii Volcano; (e), sample VM-3, pyroxenite xenolith, East Mongolia; the hump on the $M(T)$ curve is related to the oxidation of Fe-sulfides and formation of magnetite during heating the sample; (f), sample 7, Syria, Mtan Volcano, hyperbasite xenolith, with native Ni with $T_c = 390$°C; (g), (h), sample V-381, Tulun sill, Angara trap province: (h), the high-temperature segment of the curves; (i), (j), sample 2793-3, Reykjanes Ridge, basalt: (j), the high-temperature segment of the curves; (k), sample 129-17, Gulf of Mexico, basaltic glass; (l), sample 16AVR6-62, axial zone of the Mid-Atlantic Ridge, basaltic glass.

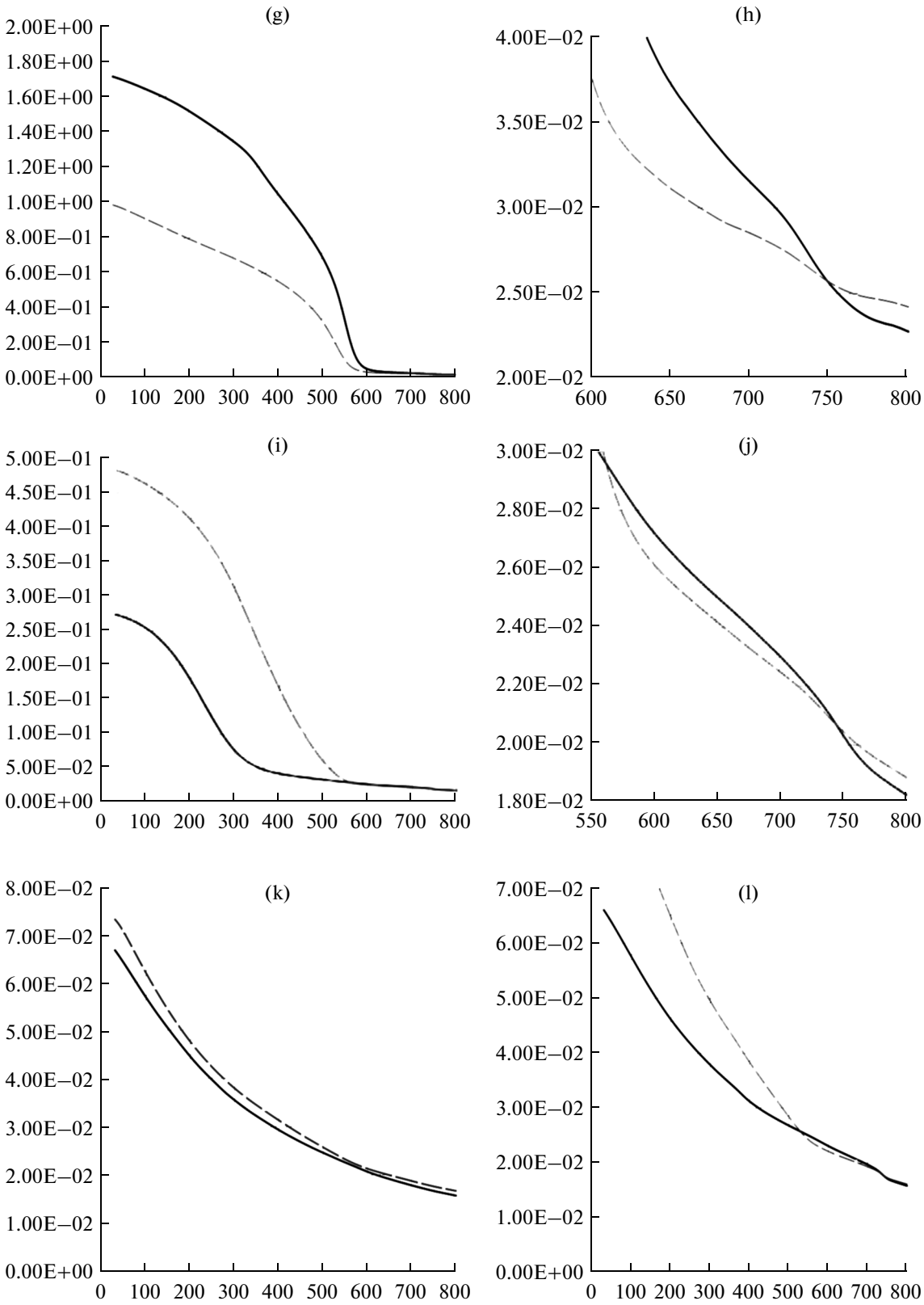
(g)
2.00E+00
1.80E+00
1.60E+00
1.40E+00
1.20E+00
1.00E+00
8.00E–01
6.00E–01
4.00E–01
2.00E–01
0.00E+00
0 100 200 300 400 500 600 700 800
(h)
4.00E–02
3.50E–02
3.00E–02
2.50E–02
2.00E–02
600 650 700 750 800
(i)
5.00E–01
4.50E–01
4.00E–01
3.50E–01
3.00E–01
2.50E–01
2.00E–01
1.50E–01
1.00E–01
5.00E–02
0.00E+00
0 100 200 300 400 500 600 700 800
(j)
3.00E–02
2.80E–02
2.60E–02
2.40E–02
2.20E–02
2.00E–02
1.80E–02
550 600 650 700 750 800
(k)
8.00E–02
7.00E–02
6.00E–02
5.00E–02
4.00E–02
3.00E–02
2.00E–02
1.00E–02
0.00E+00
0 100 200 300 400 500 600 700 800
(l)
7.00E–02
6.00E–02
5.00E–02
4.00E–02
3.00E–02
2.00E–02
1.00E–02
0.00E+00
0 100 200 300 400 500 600 700 800

**Fig. 12.** (Contd.).

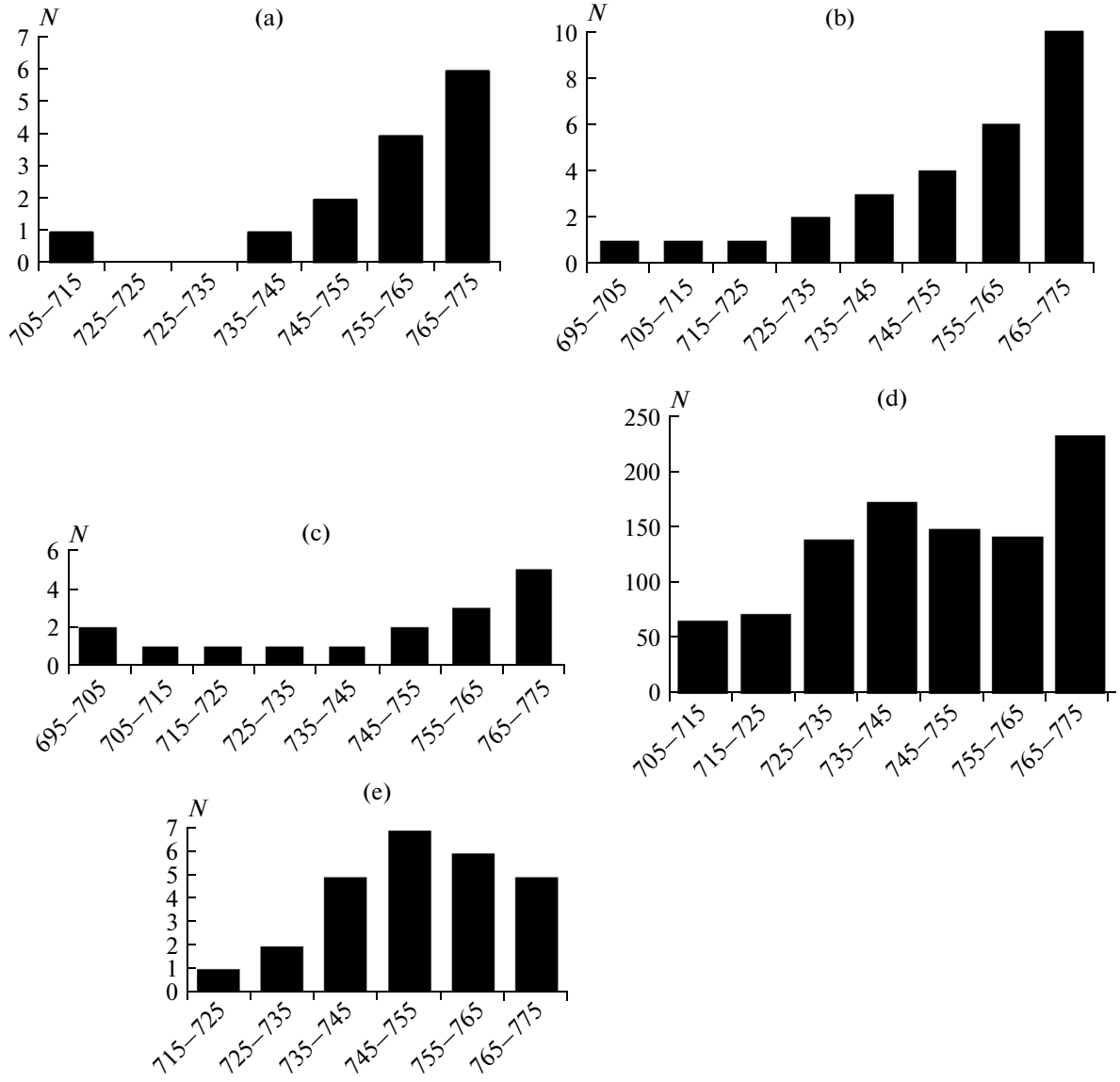


**Fig. 13.** The distribution of the Curie points (in °C) of native iron in (a) xenoliths, (b) traps, (c) oceanic basalts, (d) sediments, and (e) meteorites.

tribution of these particles in sediments. It is barely possible that native iron particles could be ubiquitously disseminated throughout all the types of the sedimentary rocks as a result of the disintegration of the hyperbasite and basalt massifs by erosion.

Let us consider one of the probable mechanisms of the global distribution of native iron, which suggests the dispersion of volcanic ash as the main driver of this phenomenon. Among the 30 studied objects of sedimentary rocks, traces of the volcanic ash (and volcanic material altogether) are only detected in two of them. (1) In the Miocene–Oligocene deposits of the Atlantics, the DSDP 386 borehole penetrated a ~160-m layer of volcanoclastic turbidites. In the samples from this interval, 22 native iron particles have been detected, which is fewer than in the neighboring terrigenous deposits (33 particles). At the same time, 50 particles of native iron are identified in the samples from borehole 391A drilled in the terrigenous carbonate rocks, in which the volcanic material is absent (Pechersky et al., 2013a). (2) In the Permian–Triassic Meishan rocks (China) there are interbeds of volcanic ash below and above the Permian/Triassic boundary. However, native iron particles are not detected in these interbeds, although they do occur in the ambient sedimentary rocks (Korchagin et al., 2010; Korchagin, 2013). In addition, native iron is not detected in the tuff layer between the trap flows (Table 1). Therefore, the volcanogenic (ash) scenario of the global dissemination of Ni-free native iron particles does not apply. The other scenarios of the terrestrial origin of these

particles (hydrothermal, metamorphic, biogenic, etc.) are even less probable as global scenarios.

Furthermore, a number of the statistical features in the distribution of native iron particles in the sediments unambiguously suggest their predominantly extraterrestrial origin (Pechersky, 2012; Pechersky and Sharonova, 2012; 2013). These features include (1) the widespread (global) occurrence of native iron particles in the sediments in the different regions of the world, from the Quaternary to Cambrian, in lacustrine, marine, and oceanic deposits, in the rocks with different lithology and under different redox conditions. The concentrations of the particles widely varies from their complete absence to 0.05%, mainly from $10^{-5}$ and $10^{-3}$%. (2) The bimodal distribution of the concentrations of native iron particles with the necessary presence of the "zero" group of the samples, in which iron particles are absent. This feature is due to the limited volume of cosmic dust precipitated onto the Earth's surface: the zero group corresponds to the intervals of the sediment which fell beyond the precipitation area of extraterrestrial native iron. The bimodal distribution of native iron particles with a mandatory zero-mode is untypical of the terrestrial magnetic minerals. (3) The absence of the correlation between the concentrations of native iron particles and the terrestrial magnetic minerals, e.g., magnetite. The appearance of this correlation is primarily due to the redeposition of extraterrestrial iron and/or it indicates their terrestrial origin. (4) The inverse proportion between the concentration of native iron particles and the rate of sedimentation. According to MPA, the majority of the particles are native iron without Ni (Table 1). Therefore, these signs of the extraterrestrial origin of iron are also valid for the Ni-free particles. (5) The predominant grain size (<100 μm, Fig. 11a) corresponds to the extraterrestrial particles which have survived upon passing through the Earth's atmosphere, whereas the upper size limit for the terrestrial particles is absent (Pechersky and Sharonova, 2013).

Thus, the extraterrestrial origin of most of the Ni-free native iron particles in the sediments is undoubted, and their global occurrence is reasonable to relate to the interplanetary cosmic dust. According to the modern understanding (e.g., McFadden et al., 2007; *Encyclopedia...*, 2012), the interplanetary cosmic dust precipitating onto the Earth originates from the asteroid belt between Jupiter and Mars. The dust comprises small particles of crushed stony material resulting from the collision of asteroids, comets, and other bodies. The close similarity of native iron in all the studied objects indicates that the formation conditions of the source planets of the cosmic dust were identical to the terrestrial conditions, or, more generally, these planets and the Earth were structurally and compositionally very similar. This uniformity is most likely to ensue from the homogeneous state of the gas-dust cloud which had given rise to the formation of the Solar System planets. The diversity of the terrestrial and meteorite rocks was created by the subsequent processes of differentiation, metamorphosis, etc.

According to the rock-magnetic model of the Earth (and, perhaps, similar planets), in the Earth's crust is an abundance of titanomagnetites and the products of their alteration (magnetites); the upper mantle rocks are almost nonmagnetic; i.e., the concentration of magnetic minerals in these rocks is below the sensitivity of the instruments measuring the magnetization (i.e., ~<$10^{-3}$%) (*Petromagnitnaya...*, 1994; Pechersky et al., 2012). We recall that the average Ti content in titanomagnetites is 8.7% in the traps, 10.5% in the oceanic basalts, and 12.5% in the basalts containing hyperbasite xenoliths. This Ti content corresponds to the depth of the last equilibrium state of basaltic magma (i.e., magma chamber) at 30–50 km (Pechersky et al., 1975), which falls in the Earth's crust and the top layers of the mantle. According to our data (Table 1), there is a clear trend in the distribution of FeNi alloys along the Earth's radius: they are clearly predominant in the lower mantle and the core where their fraction is as high as 92%, less abundant in the upper mantle where their percentage is rather low (14%), and rare in the upper mantle, making up 1–8% in the main igneous rocks, intrusive and volcanic, crystallized in the Earth's crust and on its surface. The fraction of FeNi alloys in the sediments is 18% (Table 1), which is close to hyperbasites (14%), i.e., the upper mantle rocks. The contribution of the FeNi particles is almost identical in the samples of stone and iron stone meteorites (85.3 and 87.3%, respectively) (Table 2). In the samples of the stone meteorite studied by us, the concentration of the Fe + FeNi alloys very rarely reaches 0.01%. Therefore, the samples of the stone meteorites that we had for our analysis are most likely to correspond to the bottom layers of the mantle. This is highlighted by the distribution of schreibersite (Table 2): it is typical of iron meteorites and absent in hyperbasites (xenoliths) and sediments (i.e., in the upper mantle rocks) (Pechersky et al., 2012; Pechersky and Kuzina, 2015). Following the obtained results, we may quite logically suppose that the upper mantle material disintegrates easier than the material of the lower mantle and core. Therefore, the interplanetary dust should be primarily contributed by matter from the upper mantle, whereas the material of the lower mantle and the core is mainly delivered to the Earth in the form of rather large meteorite fragments.

The close ratios of Fe + FeNi concentrations and the presence of schreibersite in the stone and iron meteorites indicate that a sharply contrasting boundary between the lower mantle and the core is absent and that there is a gradual transition instead.

The Earth's core and the crust make up 12.6 and 1.4% of the total volume of the Earth, respectively. The relative volumes of the meteorites are 1.5% (the core, iron meteorites) (Pechersky et al., 2012). This means that the core of a planet (iron meteorite) occupies a

volume that is by an order of magnitude smaller than the volume of the Earth's core. Thus, we may hypothesize that the relative volume of the core of the broken planets (a planet) was by an order of magnitude smaller than that of the Earth. This does not conflict with the percentage of native iron in the Earth, Mars, and meteorites of the asteroid belt (Hubbard, 1984). The described trend is also observed in the total Ni content in the rocks: iron meteorites contain about 10% Ni; Ni concentration in chondrites sharply drops to 0.05–1%; an even smaller average Ni concentration is present in carbonaceous chondrites; and the Fe/Ni ratio increases from 10 to 500. The global occurrence of Ni-free native iron with the Si, Al, and Mg admixtures can probably be associated with the upper mantle and crustal rocks, whose fraction is larger by a factor of a few dozen than the fraction of the core rocks. The small volume of crustal material, compared to the remaining part of a planet, explains the rare occurrence of crustal rocks among the meteorites and, in particular, their absence in the meteorites studied by us.

## CONCLUSIONS

We have generalized the results of the microprobe and thermomagnetic studies of native iron in the terrestrial sediments, mantle hyperbasites (xenoliths), oceanic and continental basalts (Siberian traps), and extraterrestrial rocks (meteorites). This analysis revealed the similarity in the compositions, grain shapes, and sizes of the particles of Ni-free native iron in all these groups of rocks. It is found that these iron particles in the sediments have mainly extraterrestrial origins, and their ubiquitous occurrence is most likely to be due to the cosmic interplanetary dust. According to the modern notions, the interplanetary dust is a product of the disintegration of a planet (or planets) in the asteroid belt. From the revealed similarity we conclude the identity of iron particle formation under the conditions of the terrestrial planets and other similar planets and, most likely, the identity of the interior structure of the planets as a result of their formation from a homogeneous gas-dust cloud at the early stage of the Solar System. This provides us with a means of tracking the single pattern of dissemination of native iron in the Earth-like planets: the concentration of Ni-free native iron in the crust is rarely above 0.001%. The number of the Ni-free native iron particles is 89% in traps and 84% in the oceanic basalts. The fraction of these particles decreases in the upper part of the mantle (it makes up 77% in the hyperbasites from the upper mantle layers); however, the concentration of native iron still rarely exceeds 0.001%. The summary characteristic of the entire upper mantle is expressed in the contribution of Ni-free iron particles in the terrestrial sediments: it is 70%, very close to hyperbasites from the top layers of the Earth's mantle. We believe that it is this material that mainly contributes to the interplanetary dust, in contrast to the matter from the lower mantle which reaches the surface of the Earth mainly in the form of relatively larger meteorite fragments. The upper mantle rocks barely contain schreibersite. In the samples of the stone meteorites, i.e., in the bottom portion of the mantle, the contribution of the Ni-free iron particles drastically drops to 14.7%, whereas the summary concentration of native iron and FeNi alloy significantly increases to 0.2–9%. Schreibersite appears in the lower horizons of the mantle, in its metal part. The contribution of Ni-free iron particles in the core of the Earth and the source planets of the cosmic dust is 12.7%; the summary concentration of native iron + FeNi alloys is 92%. Among the FeNi alloys, schreibersite makes up a significant fraction. It turns out that in terms of the amount of the Ni-free iron, a sharp boundary between the lower mantle and the core is absent. Instead, there is a gradual growth from stone meteorites to iron-stone and iron meteorites in terms of the concentration of native iron and FeNi alloys, in particular, schreibersite.

## ACKNOWLEDGMENTS

We are grateful to our colleagues for helping us with our study: G.N. Bazhenova and A.Ya. Saltykovskii for providing the samples of the mantle xenoliths from the basalts of Primor'e, Mongolia, Syria, and other localities; I. Ashchepkov for the mantle xenolith samples from the Vitim basalts; A. Latyshed for the samples of the Siberian traps; and V. Matveenkov and S. Silant'ev for the samples of the oceanic basalts.

The work was carried out according to the Russian Government's Program of Competitive Growth of Kazan Federal University and supported by grant no. 13-05-004348a of the Russian Foundation for Basic Research. TMA was funded by the grant provided to the Kazan State University for performing the state program in the field of scientific research.

## REFERENCES

Florenskii, K.P., On the initial stage of differentiation of the Earth's matter, *Geokhimiya*, 1965, no. 8, pp. 1–18.

Grachev, A.F., Kollmann, H.A., Korchagin, O.A., et al., The K/T boundary of Gams (Eastern Alps, Austria) and the nature of terminal Cretaceous mass extinction, *Abhandlungen der geologischen bundesanstalt*, Grachev, A.F., Ed., 2009, vol. 69, pp. 89–134.

Hubbard, W., *Planetary Interiors*, New York: Van Nostrand, 1984.

Korchagin, O.A., Tsel'movich, V.A., Pospelov, I.I., and Bian Qiantao, Cosmic magnetite microspherules and metallic particles near the Permian–Triassic boundary in a global stratotype section and point (stratum 27, Meishan, China), *Dokl. Earth Sci.*, 2010, vol. 432, no. 1, pp. 631–637.

Korchagin, O.A., Fossil micrometeorites, microtectites, and microcrystites: methods for studying, classification, and impact–stratigraphic scale, in *Stratigrafiya v nachale*

*XXI veka—tendentsii i novye idei. Ocherki po regional'noi geologii Rossii* (Stratigraphy at the Beginning of XXI Century: Trends and New Ideas. Essays on Regional Geology of Russia), Moscow: Geolkart-GEOS, 2013, vol. 6, pp. 112–142.

Marakushev, A.A., Granovskii, L.B., and Zinov'eva, N.G., *Kosmicheskaya petrologiya* (Cosmic Petrology), Moscow: MGU, 1992.

Markov, G.P., Pechersky, D.M., and Tsel'movich, V.A., Magnetic minerals of the Chelyabinsk meteorite, *Sol. Sys. Res.,* 2015, in press.

McFadden, L., Weissman, P.R., and Johnson, T.V., *Encyclopedia of the Solar System*, 2nd ed., San Diego: Academic, 2007.

Pechersky, D.M., Bagin, V.I., Brodskaya, S.Yu., and Sharonova, Z.V., *Magnetizm i usloviya obrazovaniya izverzhennykh porod* (Magnetism and Formation Conditions of Igneous Rocks), Moscow: Nauka, 1975.

Pechersky, D.M., Grachev, A.F., Nourgaliev, D.C., Tselmovich, V.A., and Sharonova, Z.V., Magnetolithologic and magnetomineralogical characteristics of deposits at the Mesozoic/Cenozoic boundary: Gams section (Austria), *Russ. J. Earth Sci*, 2006, vol. 8, no. 3, ES3001. doi 10.2205/2006ES000204

Pecherskii, D.M., Nurgaliev, D.K., and Sharonova, Z.V., Magnetolithologic and magnetomineralogical characteristics of sediments at the Mesozoic/Cenozoic boundary: the Koshak section (Mangyshlak peninsula), *Izv., Phys. Solid Earth*, 2006, vol. 42, no. 11, pp. 957–970.

Pecherskii, D.M., Asanidze, B.Z., Nurgaliev, D.K., and Sharonova, Z.V., Petromagnetic and paleomagnetic characterization of Mesozoic/Cenozoic deposits: the Tetritskaro section (Georgia), *Izv., Phys. Solid Earth*, 2009, vol. 45, no. 2, pp. 134–149.

Pechersky, D.M., Metallic iron and nickel in Cretaceous and Cenozoic sediments: the results of thermomagnetic analysis, *J. Environ. Prot.*, 2010, vol. 1, pp. 143–154.

Pecherskii, D.M., Nurgaliev, D.K., Fomin, V.A., Sharonova, Z.V., and Gil'manova, D.M., Extraterrestrial iron in the Cretaceous–Danian sediments, *Izv., Phys. Solid Earth*, 2011, vol. 47, no. 5, pp. 379–401.

Pechersky, D.M., *Samorodnoe zhelezo i drugie magnitnye mineraly v osadkakh: termomagnitnye priznaki kosmicheskogo proiskhozhdeniya* (Native Iron and Other Magnetic Minerals in Sediments: Thermomagnetic Signs of Extraterrestrial Origin), Saarbrücken: Palmarium Academic Publishing, 2012.

Pechersky, D.M., Markov, G.P., Tsel'movich, V.A., and Sharonova, Z.V., Extraterrestrial magnetic minerals, *Izv., Phys. Solid Earth*, 2012, vol. 48, nos. 7–8, pp. 653–670.

Pechersky, D.M. and Sharonova, Z.V., Thermomagnetic evidence of native iron in sediments, *Izv., Phys. Solid Earth*, 2012, vol. 48, no. 4, pp. 320–325.

Pechersky, D.M. and Sharonova, Z.V., A relationship between the concentration of native iron particles in sediments and the rate of their accumulation: a synthesis of thermomagnetic data, *Izv., Phys. Solid Earth*, 2013, vol. 49, no. 5, pp. 718–724.

Pecherskii, D.M., Gil'manova, D.M., Markov, G.P., Murdmaa, I.O., Nurgaliev, D.K., Tsel'movich, V.A., and Sharonova, Z.V., Native iron and other magnetic minerals in the sediments of the Northwestern Atlantic: thermomagnetic and microprobe evidence, *Izv., Phys. Solid Earth*, 2013a, vol. 49, no. 3, pp. 426–448.

Pecherskii, D.M., Gil'manova, D.M., Ivanov, E.V., Kuz'min, M.I., Markov, G.P., Nurgaliev, D.K., and Tsel'movich, V.A., Native iron in the sediments of Lake Baikal (borehole BDP-98): results of thermomagnetic analysis, *Rus. Geol. Geophys.*, 2013b, no. 9.

Pechersky, D.M., Gil'manova, D.M., Kazansky, A.Yu., Krivonogov, S.K., Nurgaliev, D.K., and Tsel'movich, V.A., Native iron in Quaternary deposits of the Darkhad Basin (northern Mongolia), *Rus. Geol. Geophys.*, 2013c, no. 12.

Pechersky, D.M. and Kuzina, D.M., Nickel-Free Iron Particles in Sediments, *Izv., Phys. Solid Earth*, 2015, in press.

*Petromagnitnaya model' litosfery* (Petromagnetic Model of the Lithosphere), Pashkevich, I.K. and Pechersky, D.M, Ed., Kiev: Naukova Dumka, 1994.

*Translated by M. Nazarenko*